High transfer coefficient niobium nano-SQUID integrated with a nanogap modulation flux line

OPEN ACCESS
IOP Publishing
Measurement Science and Technology
Meas. Sci. Technol. **32** (2021) 025001 (5pp)
https://doi.org/10.1088/1361-6501/abc454

High transfer coefficient niobium nano-SQUID integrated with a nanogap modulation flux line

Zhong Qing[1], Tsai Yuchien[2], Li Jinjin[1], Ling Hao[3], Jiang Kaili[2], Zhong Yuan[1], Cao Wenhui[1], Mingyu Zhang[1] and Wang Xueshen[1]

[1] National Institute of Metrology, Beijing 100029, People's Republic of China
[2] Tsinghua University, Beijing 100084, People's Republic of China
[3] National Physical Laboratory, Teddington, Middlesex TW11 0LW, United Kingdom

E-mail: jinjinli@nim.ac.cn and wangxs@nim.ac.cn

Received 3 August 2020, revised 9 October 2020
Accepted for publication 23 October 2020
Published 25 November 2020

Abstract

Nano-superconducting quantum interference devices (nano-SQUIDs) with high energy sensitivity and spatial resolution are essential in many applications such as single spin detection, nano-electromechanical vibration detection and microscale magnetic imaging. This paper studies a Dayem-type niobium nano-SQUID using focus ion beam milling technology. The device has two 42 nm × 60 nm nano-bridges and an integrated on-chip Nb modulation flux line located beside the SQUID loop with a 100 nm nanogap. The non-hysteretic temperature range of the nano-SQUID is about 1.4 K from 4.6 K to 6.0 K, which could broaden the operation temperature range of the device. The maximal transfer coefficient V_Φ and peak-to-peak voltage ΔV are 8.53 mV/Φ_0 and 430 μV at 4.8 K, respectively.

Keywords: nano-SQUID, focus ion beam, Josephson junctions, SQUID

(Some figures may appear in color only in the online journal)

1. Introduction

The superconducting quantum interference device (SQUID) is one of the most sensitive flux–voltage sensors. Compared to traditional microscale SQUIDs consisting of trilayer Josephson junctions, Dayem bridge nano-SQUIDs are made of weak-linked bridge junctions and have features such as higher junction current density, lower parasitic capacitance and compact size, which result in advantages of high energy sensitivity and spatial resolution. Nano-SQUIDs are therefore especially useful in applications such as single-spin detection, nano-electromechanical vibration detection, microscale magnetic imaging, the readout of inductive superconducting transition edge sensors, and so on [1–10].

The junctions in Dayem bridge nano-SQUIDs are made of nano-scale superconductor bridges. Two nanofabrication methods are commonly used to fabricate nano-SQUIDs. One is the electron beam lithography (EBL) technology method [8, 10, 11] and the other is the focused ion beam (FIB) milling technology method [12–14]. Compared to the EBL method, the FIB method is more flexible, faster, photoresist-free and sample size friendly. However, the problem with the FIB method is that there is an ion implantation issue when the ions hit the surface of the Nb superconducting film. The implantation damage leads to the quenching of the Nb bridge junction in the scale of tens of nanometers and influences the junction property. To prevent ion implantation damage, heavy metal films such as tungsten are usually deposited over the FIB etching area before FIB etching to protect the Nb film, which will be kept. Therefore, it is not easy to make high quality FIB nano-SQUIDs.

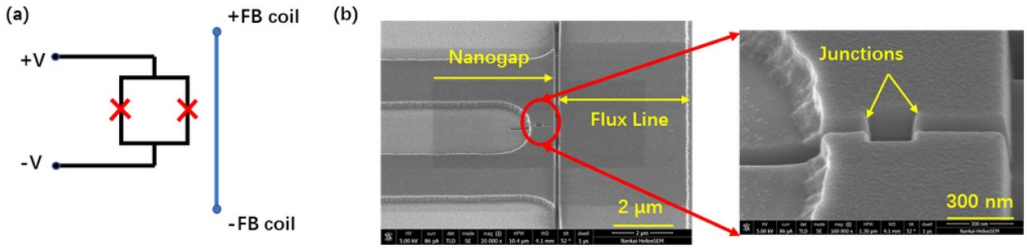

Figure 1. (a) Nano-SQUID structure diagram. (b) SEM image of one nano-SQUID. The right image is the enlarged view of the nano-SQUID.

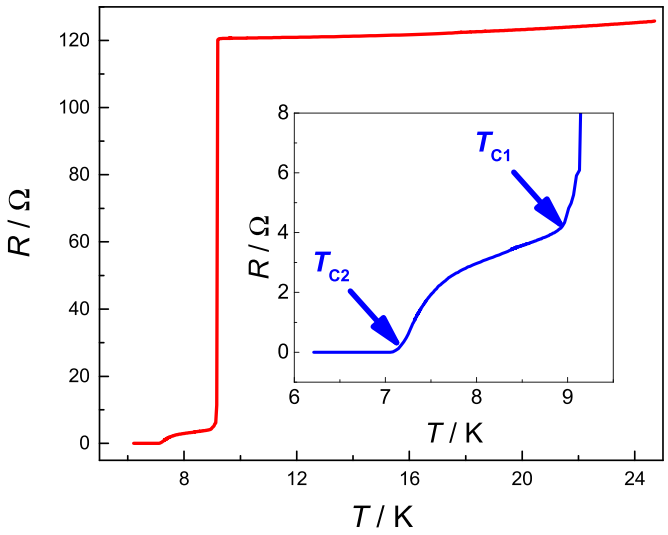

Figure 2. The *R*–*T* curve of the nano-SQUID. T_{c1} is the transition temperature of the large Nb tracks and T_{c1} is that of the nano-bridges.

In this paper, we report an FIB-nano-SQUID integrated with an on-chip magnetic flux modulation line. The voltage–flux transfer coefficient and the operational temperature range show vast superiority. Compared to the conventional external coil type of voltage–magnetic flux modulation, an on-chip modulation with a nanogap modulation flux line is used to simplify the system and improve the flux coupling. The mutual inductance between the flux line and the SQUID is about 72 mA/Φ_0. The Dayem bridge junctions and nanoscale loops of nano-SQUIDs are directly milled by FIB without any protecting layer. The maximal transfer coefficient V_Φ and peak-to-peak voltage ΔV of our nano-SQUID are 8.53 mV/Φ_0 and 430 μV at 4.8 K, respectively. The non-hysteretic temperature range of the nano-SQUID is about 1.4 K, which could broaden the operation temperature range of the device.

2. Nano-SQUID design and fabrication

Figure 1(a) shows the diagram of our nano-SQUID. The internal side length of the device is 200 nm. The width and length of the Dayem bridges are 42 nm and 60 nm, respectively. We designed a niobium flux current line beside the SQUID loop as the flux modulation coil to generate feedback flux, as shown in figure 1(a), from +FB to −FB. In order to increase the coupling effect, the distance between the flux current line and the SQUID bias line was shrunk to 100 nm.

For the fabrication process, 144 nm Nb film was firstly deposited on a SiO_2/Si substrate by a sputtering process. The background pressure of the sputtering chamber is better than 4×10^{-6} Pa. The sputtering pressure was controlled at 0.67 Pa. Common photolithography and dry etching techniques were used to form the structure with scales above 2 μm and pads for bonding. SF_6 was used to etch Nb with positive photoresist structure protection. The power and reactive pressure of the reactive ion etching were 50 W and 2 Pa respectively. FIB was then used to mill the Nb film to form the nanoscale structure of the devices, including the Dayem bridge junctions, nanoscale loops and the nanogap between the loop and the flux line, as shown in figure 1(b). In our FIB system, a gallium ion species was used and its beam energy was kept at 30 keV. The ions from the FIB beam were inevitably implanted in the junctions and consequently formed a shunt resistor. Therefore, ion dose was adjusted for different thicknesses of Nb films in order to avoid damage to the bridge junction.

3. Measurement results and discussions

The chip was adhered to a ceramic device holder using GE 7031 varnish. The holder was attached to a copper sink of which the temperature could be measured and controlled by a Lakeshore temperature controller. The electrode pads on the chip were wire-bonded to the holder by 25 μm diameter aluminum wires. The device was mounted inside a stainless steel can with the lead shield and characterized using a home-made system composed of a probestick, Keysight B2901A/B2961A current sources, a Keithley 2000 multimeter and data acquisition software.

3.1. *R–T curve*

Figure 2 shows the resistance vs temperature (*R*–*T*) curve of the nano-SQUID device made in 144 nm Nb film. The inset is the enlarged part from 6 K to 9.5 K. Clearly there are two superconducting transition temperatures T_c. The first transition at about 9.10 K (T_{c1} in figure 2) is the transition temperature of the Nb film. At this temperature, two bridge junctions are still at normal state with a few ohms resistance because of the Ga^+ implantation damage. The FIB process causes the

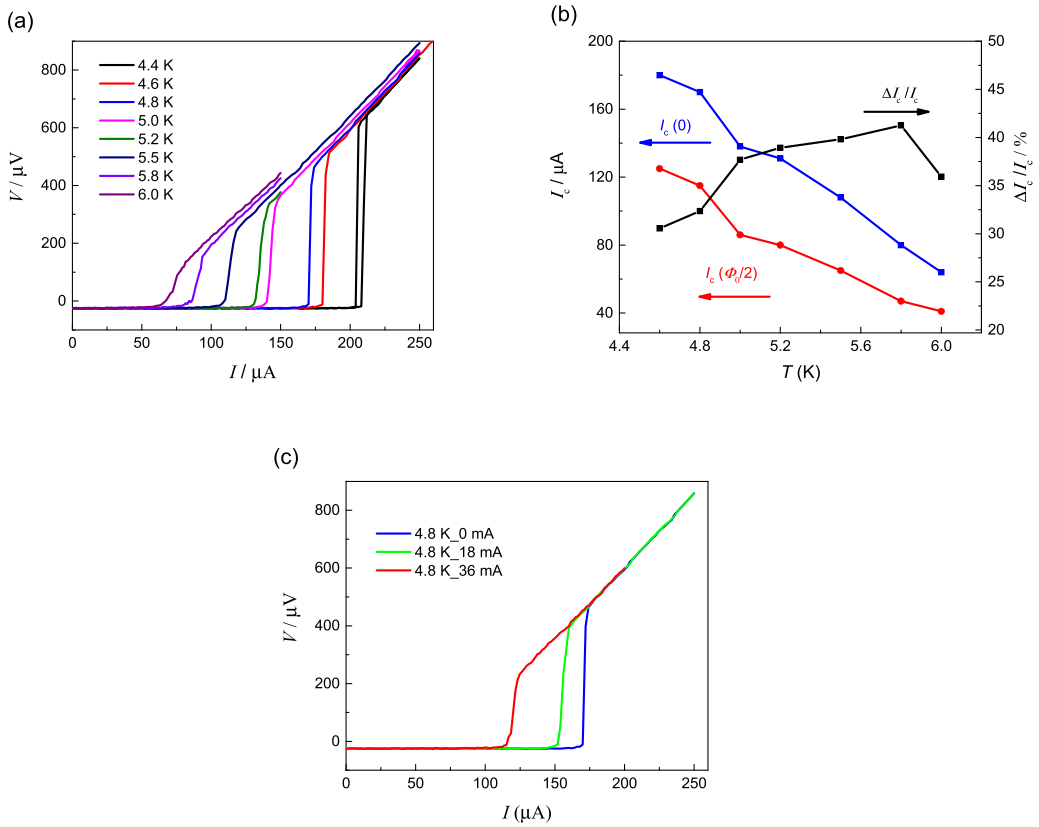

Figure 3. *I–V* curves of the the nano-SQUID (a) and corresponding critical current (b) at different temperatures. (c) *I–V* curves at 4.8 K for $0\Phi_0$, $\Phi_0/4$ and $\Phi_0/2$.

ion implantation on the surface of the Nb at the bridge region with an implantation depth of about 13 nm. Consequently, the transition temperature of Nb at the bridge region decreases. This induces the second transition temperature at about 7.05 K (T_{c2} in figure 2). This two-transition *R–T* curve is typical for the Dayem-type nano-SQUID.

3.2. *I–V curve*

Figure 3(a) shows the *I–V* curves of the nano-SQUID at different temperatures. The critical current I_c of the device decreases from 180 μA to 64 μA when the temperature increases from 4.6 K to 6.0 K. The device shows a non-hysteretic characteristic above 4.6 K. Therefore, the operating temperature range of the SQUID is about 1.4 K.

The *I–V* curve changes periodically with the external magnetic field. In this paper, an on-chip modulation flux line is applied to produce the external magnetic field. The currents of 0 mA, 19 mA and 38 mA flowing through the flux line produce fluxes of $0\Phi_0$, $\Phi_0/4$ and $\Phi_0/2$, respectively. Figure 3(c) shows the *I–V* curve at 4.8 K for $0\Phi_0$, $\Phi_0/4$ and $\Phi_0/2$, and the corresponding critical currents I_c in these cases are 170 μA, 152 μA and 115 μA. I_c decreases nonlinearly with increasing flux from 0 to $\Phi_0/2$. The flux modulating depth $\Delta I/I_c$ is 32.4% at 4.8 K [15]. The black line in figure 3(b) shows the change of the flux modulating depth $\Delta I/I_c$ with the temperature. The maximum value is 41.5% at 5.8 K.

3.3. *V–Φ curve*

The voltage across the nano-SQUID was measured with external magnetic flux at different biased current I_b and temperatures. Figure 4(a) illustrates the *V–Φ* curves with different I_b from 110 to 170 μA at 4.8 K. ΔV is defined as the peak-to-peak modulation voltage. The SQUID transfer coefficient V_Φ is the maximum absolute value of $\partial V/\partial\Phi$. $V_{\Phi+}$ and $V_{\Phi-}$ represent the V_Φ at the rising and falling edge of the *V–Φ* curve. The V_Φ value reflects the sensitivity of the SQUID to magnetic flux changes. The higher the value, more sensitive the SQUID device is. Figure 4(b) illustrates ΔV, $V_{\Phi+}$ and $V_{\Phi-}$ as function of I_b. It shows that ΔV increases with I_b from 110 to 160 μA and then decreases. $V_{\Phi+}$ and $V_{\Phi-}$ have the same trend, as expected. From the data we can derive that the 160 μA bias current corresponds to the best working point at this temperature. The optimal bias current is chosen to be the point where $V_{\Phi+}$ is the best. At this working condition, $V_{\Phi+}$ and ΔV of this device are 8.53 mV/Φ_0 and 430 μV, respectively. This result is much better than the 2D Dayem bridge devices reported in the literature, with the transfer coefficient in the range of 0.1–2.5 mV/Φ_0 [8, 11–13].

Figure 5(a) illustrates the V–Φ curves of the optimal transfer characteristic at different temperatures from 4.4 K to 6.0 K. The corresponding optimal bias current at each temperature is shown on the upper-right corner of figure 5(a). When the temperature increases, the optimum of the bias current I_b decreases. Figure 5(b) illustrates the change of the transfer

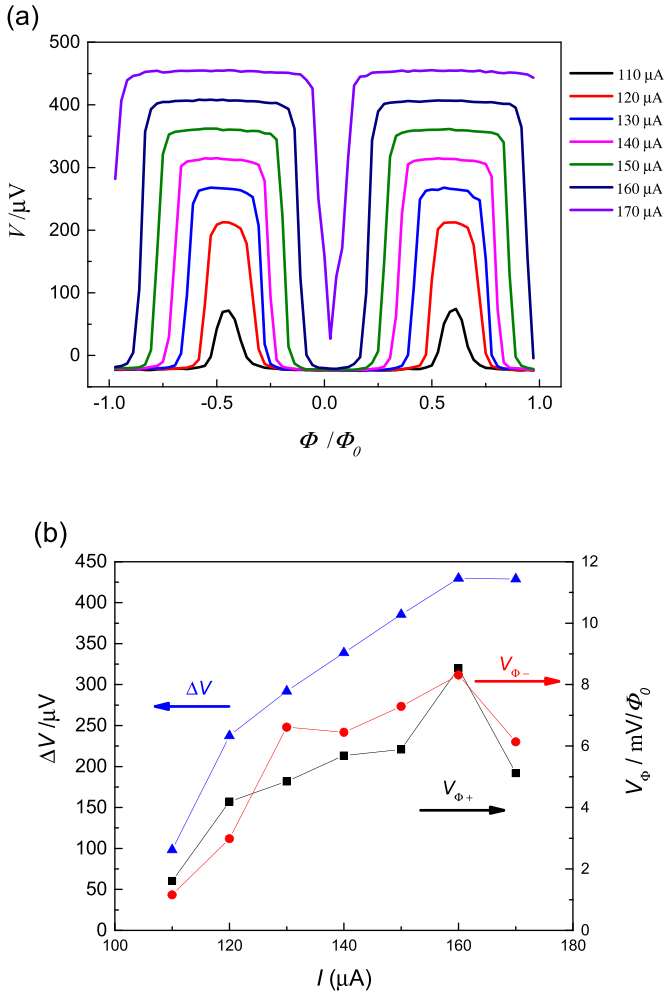

Figure 4. (a) V–Φ curves and (b) transfer coefficient $V_{\Phi+}$, $V_{\Phi-}$ and the peak-to-peak voltage ΔV as a function of biased current at 4.8 K.

coefficient $V_{\Phi+}$ and the peak-to-peak voltage ΔV at optimum bias current as a function of temperature. $V_{\Phi+}$ decreases with temperature nonlinearly, while ΔV decreases linearly with the temperature.

The effective area of the nano-SQUID needs to be estimated since it is usually not the nominated one. The effective area A_{eff} can be estimated by equation $\Phi_0 = B \times A_{\text{eff}}$. We use the PPMS (Physical Property Measurement System) to generate certain magnetic field B. The SQUID output voltage changes periodically. Each period corresponds to 1 Φ_0. 5.5 mT is needed for 1 Φ_0. So, the estimated A_{eff} is 0.36 μm^2, which is almost 10 times the nominated loop size. There are two reasons. The first reason is due to the change of the effective length of the SQUID hole. One change comes from the penetration depth effect. For the 144 nm thickness Nb film and normalized working temperature (T/Tc) of 0.53, the penetration depth at each side of the loop is about 96 nm [16]. Therefore, the effective side length of the SQUID loop now expands to about 392 nm. The second reason is the flux focusing effect. The SQUID's wide Nb loop and bank will expel magnetic flux into the hole and consequently cause the real magnetic field to be higher than the nominal one. Considering these two factors, the effective area of the SQUID can be calculated using [17]:

$$A_{\text{eff}} = \gamma_{\text{A}} \cdot d \cdot (d+2w)\,\gamma_{\text{A}} = 1 - 0.68/(d/w+2.07)^{1.75},$$

the effective side length $d \approx 392$ nm and washer width $w \approx 300$ nm. A_{eff} is calculated to be 0.357 μm^2, which is very close to the estimated A_{eff} of 0.36 μm^2.

This small effective area induces a very high spatial resolution, but also reduces the capture ability of the magnetic flux. A large magnetic field intensity is needed for the device to collect a quantum flux Φ_0. The magnetic field intensity generated by a long straight wire is proportional to the current and inversely proportional to the distance. A large current will cause the quenching effect of the modulation line, which will affect the operation of the nano-SQUID. When the distance is reduced by one order of magnitude from 1 micron to 100 nanometers, the current inducing the same magnetic field intensity is reduced by one order of magnitude, and the coupling between the SQUID and the modulation flux line will be increased. This will significantly increase the coupling between the SQUID and the modulation flux line, and may make the SQUID operate in a flux-locked loop mode.

The theoretic intrinsic flux noise is estimated according to the following equation [1, 18]:

$$S_{\Phi}^{1/2} \approx \left(\frac{4\,(1+\beta_L)\,\Phi_0 k_{\text{B}} TL}{I_c R_{\text{n}}}\right)^{\frac{1}{2}},$$

where k_{B} is the Boltzmann constant, T is the working temperature and the normal resistance of the SQUID's R_{n} is about 4.9 Ω from the I–V curve. L is the total inductance of the SQUID, which is the sum of the bridge inductance and the loop inductance. The evaluation is performed at 4.8 K with maximum critical current of 170 μA. For our design, the bridge inductance is 7.4 pH and the loop inductance 0.3 pH. The calculated $S_{\Phi}{}^{1/2}$ is 0.037 μΦ$_0$/Hz$^{1/2}$ when $\beta_L \to 1$. The actual measurement results will be one to two orders of magnitude larger than the theoretical calculation.

4. Conclusion

A Dayem-type niobium nano-SQUID with 42 nm × 60 nm nano-bridges and a loop of which the side length was 200 nm was fabricated using FIB milling and characterized. At 4.8 K, the device's flux modulating depth is 32.4%. The maximal transfer coefficients V_{Φ} and ΔV are as large as 8.53 mV/Φ_0 and 430 μV with 160 μA bias current, respectively.

Acknowledgments

We are very grateful to Wu Wei, an engineer of Nankai University, for his fine processing of our devices with FIB, and He

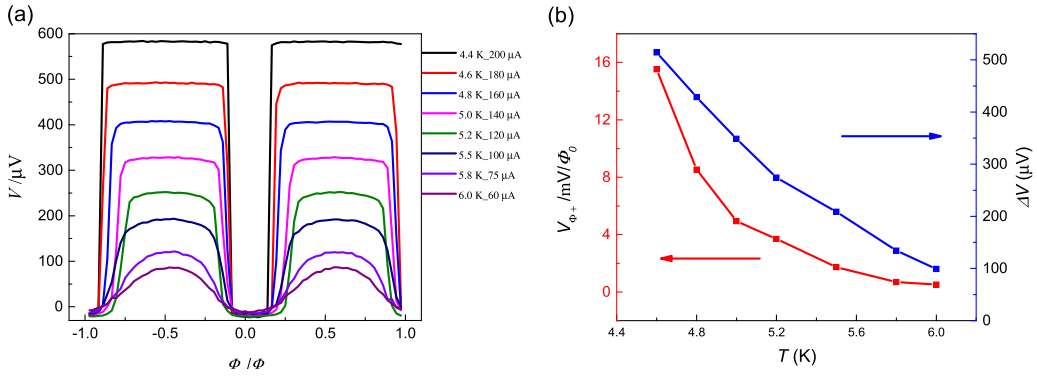

Figure 5. (a) Optimal V–Φ curves at different temperatures. (b) Transfer coefficient $V_{\Phi+}$ and the peak-to-peak voltage ΔV at optimum bias current as a function of temperature.

Zhongdu, an engineer from FEI company, for his helpful discussion. This work was supported by the National Key R&D Program of China (2017YFF0206105) and the National Natural Science Foundation of China (61701470).

ORCID iD

Zhong Yuan https://orcid.org/0000-0001-7638-7000

References

[1] Clarke J and Braginski A I 2004 *The SQUID Handbook: Fundamentals and Technology of SQUIDs and SQUID Systems, I* (Weinheim: Wiley)
[2] Wernsdorfer W 2009 From micro- to nano-SQUIDs: applications to nanomagnetism *Supercond. Sci. Technol.* **22** 064013
[3] Foley C P and Hilgenkamp H 2009 Why NanoSQUIDs are important: an introduction to the focus issue *Supercond. Sci. Technol.* **22** 064001
[4] Martinez-Perez M J and Koelle D 2017 NanoSQUIDs: basics & recent advances *Phys. Sci. Rev.* **2** 20175001
[5] Hao L and Granata C 2017 Recent trends and perspectives of nanoSQUIDs: introduction to 'Focus on nanoSQUIDs and their applications' *Supercond. Sci. Technol.* **30** 050301
[6] Vasyukov D *et al* 2013 A scanning superconducting quantum interference device with single electron spin sensitivity *Nat. Nanotechnol.* **8** 639–44
[7] Drung D, Storm J, Ruede F, Kirste A, Regin M, Schurig T, Repollés A M, Sesé J and Luis F 2014 Thin-film microsusceptometer with integrated nanoloop *IEEE Trans. Appl. Supercond.* **4** 1600206
[8] Granata C, Esposito E, Vettoliere A, Petti L and Russo M 2008 An integrated superconductive magnetic nanosensor for high-sensitivity nanoscale applications *Nanotechnology* **19** 275501
[9] Bechstein S *et al* 2015 Design and fabrication of coupled NanoSQUIDs and NEMS *IEEE Trans. Appl. Supercond.* **25** 1602604
[10] Russo R, Granata C, Esposito E, Peddis E, Cannas C and Vettoliere A 2012 Nanoparticle magnetization measurements by a high sensitive nano- superconducting quantum interference device *Appl. Phys. Lett.* **101** 122601
[11] Lam S K H and Tilbrook D L 2003 Development of a niobium nanosuperconducting quantum interference device for the detection of small spin populations *Appl. Phys. Lett.* **82** 1078
[12] Troeman A G P, Derking H, Borger B, Pleikies J, Veldhuis D and Hilgenkamp H 2007 NanoSQUIDs based on niobium constrictions *Nano Lett.* **7** 2152–6
[13] Hao L, Macfarlane J C, Gallop J C, Cox D, Beyer J, Drung D and Schurig T 2008 Measurement and noise performance of nano-superconducting-quantum-interference devices fabricated by focused ion beam *Appl. Phys. Lett.* **92** 192507
[14] Matsumoto T, Kashiwaya H, Shibata H, Takayanagi H, Nomura S and Kashiwaya S 2011 Fabrication of weak-link Nb-based nano-SQUIDs by FIB process *Physica* C **471** 1246–8
[15] Wang H, Yang R T, Li G Q, Wu L, Liu X Y, Chen L, Ren J and Wang Z 2018 Noise of dc-SQUIDs with planar sub-micrometer Nb/HfTi/Nb junctions *Supercond. Sci. Technol.* **31** 055015
[16] Wang R F, Zhao S P, Xu F Z, Chen G H and Yang Q S 2002 Data analysis in the measurement of superconductor magnetic field penetration depth *Acta Phys. Sin.* **51** 889–93
[17] Drung D 2016 *IEEE/CSC & ESAS Superconductivity News Forum* (global edn)
[18] Tinkham M 1996 *Introduction to Superconductivity* 2nd edn (New York: McGraw-Hill)